AFRL-RY-WP-TP-2013-0031

POWER SCALING OF CW AND PULSED IR AND MID-IR OPSLs (POSTPRINT)

Robert Bedford

Optoelectronic Technology Branch
Aerospace Components & Subsystems Division

J. V. Moloney, J. Hader, T .L. Wang, Y. Ying, Y. Kaneda, and J. M. Yarbough

Univerity of Arizona

T. J. Rotter, G. Balakrishnan, and C. Hains

University of New Mexico

S. W. Koch, W. Stolz, and B. Kunert

University of Marburg

JANUARY 2013
Interim

AIR FORCE RESEARCH LABORATORY
SENSORS DIRECTORATE
WRIGHT-PATTERSON AIR FORCE BASE, OH 45433-7304
AIR FORCE MATERIEL COMMAND
UNITED STATES AIR FORCE

REPORT DOCUMENTATION PAGE

Form Approved
OMB No. 0704-0188

1. REPORT DATE *(DD-MM-YY)*	2. REPORT TYPE	3. DATES COVERED *(From - To)*
January 2013	Technical Paper	1 October 2009 – 11 January 2011

4. TITLE AND SUBTITLE
POWER SCALING OF CW AND PULSED IR AND MID-IR OPSLs (POSTPRINT)

5a. CONTRACT NUMBER
In-house

5b. GRANT NUMBER

5c. PROGRAM ELEMENT NUMBER
62204F

6. AUTHOR(S)
Robert Bedford (AFRL/RYDH)
J. V. Moloney, J. Hader, T .L. Wang, Y. Ying, Y. Kaneda, and J. M. Yarbough (Univerity of Arizona)
T. J. Rotter, G. Balakrishnan, and C. Hains (University of New Mexico)
S. W. Koch, W. Stolz, and B. Kunert (University of Marburg)

5d. PROJECT NUMBER
2002

5e. TASK NUMBER
IH

5f. WORK UNIT NUMBER
[illegible]

7. PERFORMING ORGANIZATION NAME(S) AND ADDRESS(ES)
Optoelectronic Technology Branch
Aerospace Components & Subsystems Division
Air Force Research Laboratory, Sensors Directorate
Wright-Patterson Air Force Base, OH 45433-7320
Air Force Materiel Command, United States Air Force

University of Arizona
University of New Mexico
University of Marburg

8. PERFORMING ORGANIZATION REPORT NUMBER
AFRL-RY-WP-TP-2013-0031

9. SPONSORING/MONITORING AGENCY NAME(S) AND ADDRESS(ES)
Air Force Research Laboratory
Sensors Directorate
Wright-Patterson Air Force Base, OH 45433-7320
Air Force Materiel Command
United States Air Force

Air Force Office of Scientific Research AFOSR
875 North Randolph Street, Suite 325, Room 3112
Arlington, VA 22203-1768

10. SPONSORING/MONITORING AGENCY ACRONYM(S)
AFRL/RYDH

11. SPONSORING/MONITORING AGENCY REPORT NUMBER(S)
AFRL-RY-WP-TP-2013-0031

12. DISTRIBUTION/AVAILABILITY STATEMENT
Approved for public release; distribution unlimited.

13. SUPPLEMENTARY NOTES
Journal article published in Proc. SPIE 7919, 79190S-1-10, 2011. ©2011 SPIE. The U.S. Government is joint author of the work and has the right to use, modify, reproduce, release, perform, display or disclose the work. PAO Case Number 88ABW-2011-0083, Clearance Date 11 January 2011. Report contains color.

14. ABSTRACT
We present an overview of the quantum design, growth and lasing operation of both IR and mid-IR OPSL structures aimed at extracting multi-Watt powers CW and multi-kW peak power pulsed. Issues related to power scaling are identified and discussed. The IR OPSLs based on InGaAs QW bottom emitters targeted at wavelengths between 1015nm and 1040nm are operated in CW mode (yielding a maximum power of 64W) and pulsed (peak power of 245W). The mid-IR top emitter OPSLs designed to lase at 2μm are based on a novel lattice mismatched growth using InGaSb QWs and yield a maximum peak power of 350W pulsed.

15. SUBJECT TERMS
Semiconductor, lasers

16. SECURITY CLASSIFICATION OF:			17. LIMITATION OF ABSTRACT:	18. NUMBER OF PAGES	19a. NAME OF RESPONSIBLE PERSON (Monitor)
a. REPORT	b. ABSTRACT	c. THIS PAGE			Robert Bedford
Unclassified	Unclassified	Unclassified	SAR	12	19b. TELEPHONE NUMBER *(Include Area Code)* N/A

Invited Paper

Power Scaling of CW and Pulsed IR and mid-IR OPSLs

J. V Moloney[a,b], J. Hader[a,b], T.-L. Wang[b], Yi. Ying[b], Y. Kaneda[b], J. M. Yarborough[b], T. J Rotter[c], G. Balakrishnan[c], C. Hains[c], S.W. Koch[d], W. Stolz[d], B. Kunert[d],R. Bedford[e]
[a]Nonlinear Control Strategies Inc, 3542 N. Geronimo Ave, Tucson, AZ 87505
[b]College of Optical Sciences, University of Arizona, Tucson, AZ 85721
[c]Center for High Technology Materials, University of New Mexico, Albuquerque, NM 87106
[d]Physics Department, University of Marburg, 35032 Marburg, Germany
[e]Air Force Research Laboratory, Wright Patterson Air Force Base, Ohio

ABSTRACT

We present an overview of the quantum design, growth and lasing operation of both IR and mid-IR OPSL structures aimed at extracting multi-Watt powers CW and multi-kW peak power pulsed. Issues related to power scaling are identified and discussed. The IR OPSLs based on InGaAs QW bottom emitters targeted at wavelengths between 1015nm and 1040nm are operated in CW mode (yielding a maximum power of 64W) and pulsed (peak power of 245W). The mid-IR top emitter OPSLs designed to lase at 2μm are based on a novel lattice mismatched growth using InGaSb QWs and yield a maximum peak power of 350W pulsed.

1. INTRODUCTION

The design and optimization of virtually every operational aspect of a semiconductor laser or amplifier requires a quantitative knowledge of the semiconductor material optical response. Important ingredients of the optical material properties are absorption/gain and refractive index, as well as radiative and nonradiative recombination processes. All of these quantities critically influence semiconductor amplifier or laser performance. For vertical external cavity surface emitting structures (VECSELs), this quantum design input[1] proves critical as the resonant periodic gain (RPG) structure needs to be controlled to a high degree of accuracy during growth to achieve maximum power extraction. The quantum design approach provides for intervention at the wafer growth level to correct for drift in growth over the very long times required to grow the relatively thick RPG and DBR. As VECSEL output power rollover occurs at elevated temperatures, thermal management plays a central role in ultimately pushing CW power extraction to the hundred Watt level and beyond. Additionally, VECSEL chip mounting and etching (for bottom emitters) significantly impact power extraction.

Thermal management plays a central role in increasing the operation power of a VECSEL chip and two methods for heat extraction are typically employed. The more commonly employed approach is to use a transparent, low birefringent single crystal diamond heat spreader to extract the heat from the nearby "hot' RPG region. In this approach the structure is typically grown as a "top emitter" with the DBR grown first followed by the RPG multiple QW layers. In some instances the thick GaAs or GaSb substrate may be lapped down to around 100μm to facilitate some heat removal from the bottom of the chip. While this approach would suggest the best mode for power scaling, results so far are typically reported to be below or around 10W maximum. The other approach is more involved as it involves growing the active RPG region first on the GaAs or GaAb substrate, mounting it on a CVD diamond heat spreader and completely removing the substrate via an appropriate chemical etch process. This approach has been adopted by Coherent[2], our group and a few others.

Vertical External Cavity Surface Emitting Lasers (VECSELs), edited by Ursula Keller, Proc. of SPIE
Vol. 7919, 79190S · © 2011 SPIE · CCC code: 0277-786X/11/$18 · doi: 10.1117/12.874201

In this paper we will review progress made so far in our attempts to power scale VECSEL chips in both IR and mid-IR regions of the spectrum. The IR VECSELs consist of InGaAs QWs with GaAsP barriers, grown as bottom emitters on a GaAs substrate. Section 2 details our progress in utilizing the quantum design approach to optimize wafer growth and presents results for CW and pulsed operation of these VECSELs. Section 3 repeats the process for mid-IR VECSELs lasing at 2μm and the top emitter wafer growth is implemented via a novel lattice mismatched "interfacial-misfit array" (IMF) method pioneered at the Center for High Technology Materials, University of New Mexico[3]. Details of this growth method are given elsewhere in this proceedings. Essentially it allows us grow GaSb RPG and DBR regions on a GaAs substrate. The latter has many advantages including higher thermal conductivity (for top emitters) and ease of substrate removal for future bottom emitters.

2. POWER SCALING IR CW VECSEL BOTTOM EMITTERS

In this section, we discuss a series of devices, designed using the commercial SimuLase™ software[4], where we modify the semiconductor epitaxial growth and /or AR coat the chip for pump reflection while retaining high reflectivity at the signal or to reduce both pump and signal reflection. In the first device below, the RPG MQW stack was grown on a GaAs/AlAs DBR[5]. This has the drawback that the DBR mirror can absorb the excess 808nm pump light in the GaAs layer thereby adding further heating to the chip and preventing a double pas pump arrangement. This structure was the first growth on a new MOVPE reactor and it was not feasible to grow a pump transparent AlGaAs DBR at the time. Despite this drawback, we report a record power of 64W multimode at 1040nm using an 808nm pump spot of 810μm diameter. The second structure grown on an AlGaAs DBR allows us to recycle the pump light and significantly improve the slope efficiency.

The device contains ten InGaAs-wells between strain compensating and pump absorbing GaAsP barriers. The barrier thickness has been chosen such that the wells are at the anti-nodes of the 1040nm lasing mode at high power operation, i.e. at an internal temperature of about 375K. This active region is grown on a GaAs/AlAs distributed Bragg reflector (DBR) with 21 repeats. The resulting DBR stop band of high reflectivity is centered around 1035nm at room temperature. The device is capped by a carrier confining InGaP window layer.

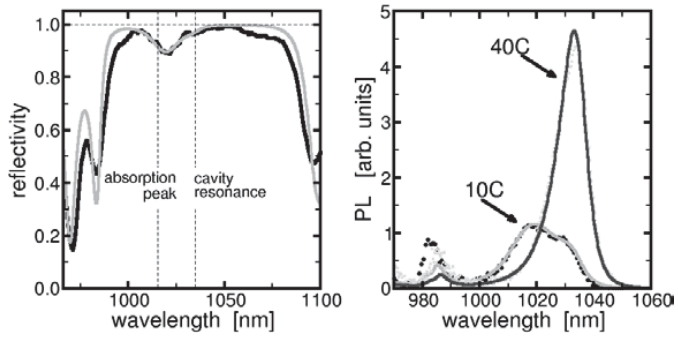

Figure 1. Left: Theoretically calculated (grey) and experimentally measured (black) reflectivity at 295K. 'Absorption peak' marks the wavelength of the quantum well excitonic absorption edge. 'Cavity resonance' marks the wavelength of the sub-cavity resonance in absence of quantum well absorption. Right: theoretically calculated (lines) and experimentally measured (symbols) surface PL spectra at heat sink temperatures of 10C and 40C.

The quantum wells and layer thicknesses were designed using the OPSL design software SimuLase[1] . This included the calculation of the quantum well gain to ensure it is maximal at 1040nm under high power

operation as well as the calculation of surface emitted photo luminescence and reflectivity spectra for quality control of the grown device. For more details on the microscopic many-body calculations involved in this design and analysis approach see Refs. 1,4.

Fig. 1 shows a comparison between the calculated and experimentally measured reflection and surface-PL spectra. The good agreement confirms highly accurate growth. For the shown agreement we only had to assume minor deviations from the design, like, that the quantum well absorption/gain is at about 2meV lower energies than designed and a 0.5% error in the thickness of the DBR layers.

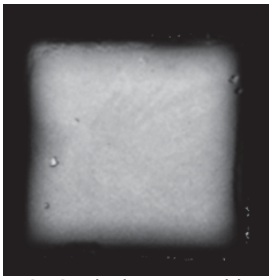

Figure 2. Acoustic microscope image of the OPSL device. No voids are present at the center of the device but only one void around the left edge.

To efficiently remove the heat from the gain structure, the semiconductor chip cleaved from the wafer is soldered with indium with a thickness of 8 microns to a 500-μm thick CVD diamond heatspreader with high thermal conductivity ($1800 WK^{-1}m^{-1}$) with the DBR side down. This soldering was done in vacuum to prevent unwanted void formation during bonding. Acoustic microscope imaging (Fig. 2) shows that the resulting OPSL device has a void-free solder joint supporting efficient heat removal from the OPSL during high power operation.

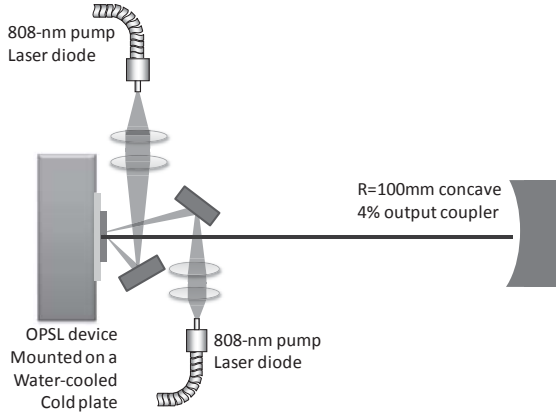

Figure 3. OPSL experiment setup. Two 808 nm pump beams are imaged on the OPSL device simultaneously for a total pump power over 270 W. A 6 cm linear cavity with concave output coupler with 10 cm radius of curvature results in a mode with 250 μm diameter.

After In-soldering, the GaAs substrate is then etched away by selective chemical etching. This etching process, particularly the selectivity of the etch rate between the GaAs substrate and InGaP window layer is critical since the thickness of the window layer needs to be well controlled in order to maintain the micro-cavity resonance at the designed location. Moreover, a homogeneous and flawless surface is required for power scaling experiments where the pump spot size is scaled. Small surface defects cause inefficient output

generation and can lead to damage during high power operation. A surface scanning image taken with a Veeco NT 9800 optical profiler shows that the surface roughness is around +/-10 nm within a 1.35 mm diameter circle.

The experimental setup of the high power OPSL operation is shown in Fig.3. The OPSL device is mounted on a water-cooled copper cold plate. The CVD diamond heatsink is clamped to the cold plate with a piece of 50 μm thick indium foil in between. Two 808-nm pump beams from multi-mode, fiber-coupled diode stacks are expanded and imaged onto the OPSL device at an 18° angle of incidence to pump a spot with 810 μm diameter. The two pump beams are adjusted to overlap for multiplexed pumping. Since the OPSL device is not antireflection coated it has approximately 30% Fresnel reflection. A 6 cm linear cavity with concave output coupler with 10 cm radius of curvature was used and it provided a lasing mode size of 250 μm in diameter on the OPSL device. The transmission of the output coupler used here is 4%. The micro-cavity resonance enhances the effective gain of the OPSL device, allowing the use of substantially higher output coupling compared to previously published results.

In this research project, we have reported a near-diffraction limited output up to 23.8 W from a single OPSL device pumped by a 550-μm big incident beam in Ref. 5. Furthermore, 40.7 W of multimode output from a 700-μm scaled pump spot is also reported. With an improved device processing, we were able to pump the OPSL device with a larger pump spot up to 810 μm. The output performances are shown in Fig. 4. Laser threshold is around 17 W and 22 W of net pump power at 10°C and 0°C respectively. Recoverable thermal roll-over, which is defined as the power level at which the output power stops to increase with higher pump power, occurred at an output power 57 W when the heat sink temperature was maintained at 10°C and 64 W at 0°C. 40% of slope efficiency and 35% of maximum optical efficiency was obtained at 0°C. Because of the wavelength filtering effect of the micro-cavity, the output spectrum is fairly narrow, around 2-3 nm wide. The center wavelength was around 1030 nm at threshold and 1040 nm at roll-over.

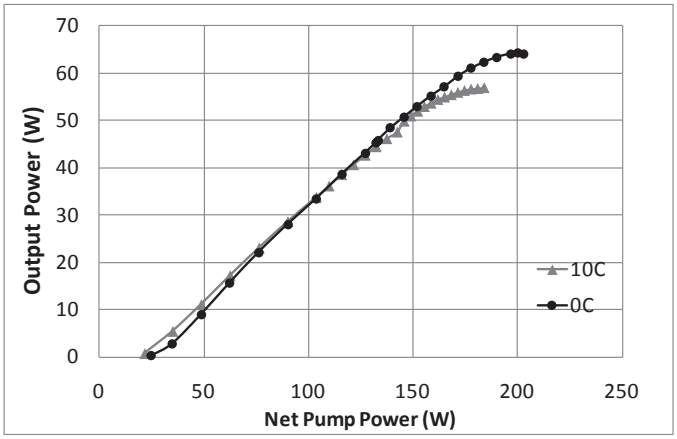

Figure 4. OPSL performance at 10°C and 0°C. The maximum output powers obtained are 57 W and 64 W at 10°C and 0°C, respectively. The slope efficiency is around 40%.

In order to have sufficient pump power we pumped a single OPSL device with two diode lasers at the same time. However, these two lasers used in the experiment are not identical. Laser A has a 200-μm diameter output with top-hat profile and laser B has a 400-μm diameter output with much higher intensity in the center of transverse profile. During the experiment, we found that the output power rolled over earlier when we pumped the OPSL device with maximum power of laser B which is 195 W and less power from laser A. As the result, pumping the OPSL device mainly with laser A gives a higher roll-over power which we show in Fig. 4. The pump profile not only affects the OPSL efficiency but also the local temperature in high power operation. This issue is discussed elsewhere in these proceedings.

The result reported here is a record continuous wave operation of OPSL at 1040 nm. This is despite the fact that the GaAs in the AlAs/GaAs DBR absorbs the pump at 808nm – our microscopic calculations indicate that around 80% of the net pump power (minus the surface reflected component) is absorbed in the barriers and the remaining 20% is absorbed in the DBR.

The structure investigated next is designed to lase around 1010nm. It contains a DBR that is transparent for the pump light with 22 $Al_{0.2}Ga_{0.8}As$/AlAs repeats. The active RPG region again consists of ten InGaAs wells positioned at the anti-nodes of the lasing mode under the expected high power operating conditions. The wells are separated by pump absorbing and strain compensating GaAsP barrier layers. The sub-cavity is capped by a carrier confining InGaP layer. This structure is also grown as a bottom emitter, i.e. with the DBR on top. The chip is soldered with the DBR side to a diamond heat spreader, which is mounted on a copper heatsink. The substrate is removed using the GaAsP cap layer as an etch stop. The thermal resistivity for this configuration is calculated to be about 0.8 mm^2K/W.

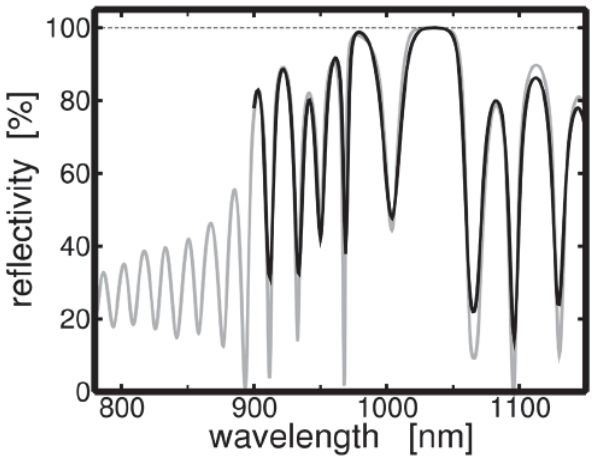

Figure 5 Reflection of the 1010nm OPSL without AR-coating at 70°C. Black:Expt. Grey:theory

This device further differs from the 1040nm OPSL discussed above in that we metalize the semiconductor chip with a thin 5nm Chromium adhesion layer and a 100nm Au layer. The idea is to double pass a finite fraction of the pump light (about 50%) passing through the transparent DBR. Fig. 5 shows a comparison between experimentally measured and calculated reflectivity spectra for the 1010nm VECSEL. The data shown here is for a temperature of 70°C where the dip in the cavity resonance is found to be the deepest. This indicates that at this temperature the quantum well absorption and the RPG cavity resonance are aligned. This also indicates that at about this temperature the maximum of the quantum well gain and the cavity resonance will be aligned which should result in optimum high power performance.

The device has been designed to have a spectral detuning between cavity resonance and quantum well gain at room temperature such that they align under maximum high power operating conditions which are assumed to be reached for an internal temperature of about 100°C. The calculations show that under high power conditions the maximum of the gain is at about 10 nm shorter wavelengths than the absorption bandedge which is seen in the low excitation reflectivity measurements. This means that gain and cavity resonance align at about 25 degree higher temperatures than where the minimum of the cavity resonance dip is observed. Thus, the detuning in the realized device is in very good agreement with the design.

In order to find agreement between the calculated and measured DBR stop-band reflectivity we had to assume that there is a drift in the thickness of the AlAs DBR layers of about 1%. Without this assumption the calculated DBR reflectivity would fall off too fast on the low or high wavelength end of stop band and significant deviations in the reflectivity fringes outside the stop-band are found.

Optical modes outside the DBR stop band are not localized in the active region but delocalized with significant amplitude throughout all layers. Thus, the reflectivity at these wavelengths is also a sensitive measure to the accuracy of cladding and metallization layers. Here we find that the top most Chromium metallization layer which is followed by a thick Gold layer has a thickness of about 7 nm instead of the intended 5 nm. Without this assumption the fringes of the reflectivity outside the stop band would be significantly higher than what is found in the measured spectra. It will also be shown later that input-output power characteristics for this device support the assumption of the thicker Chromium layers.

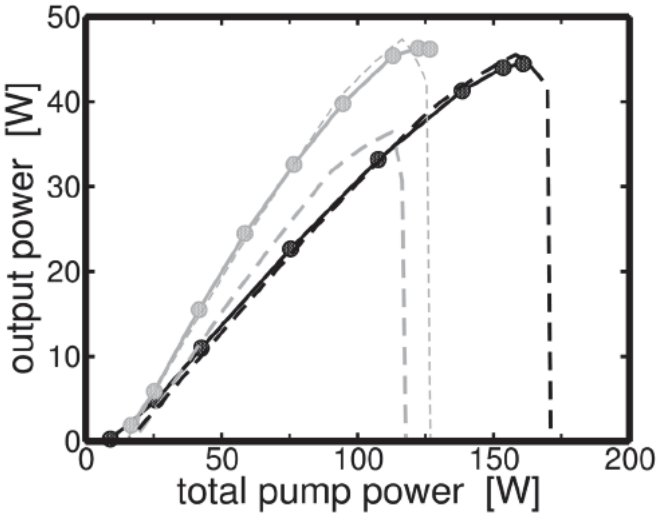

Figure 6. Output power versus total pump power for the 1010nm OPSL. Solid Black curve with circles: Experiment before coating. Solid Grey curve with circles: Experiment with pump AR-coating. Bold dashed black: Theory before coating. Bold dashed grey: Theory with pump AR-coating.

Fig. 6 shows the extracted power from the 1010nm OPSL with a thick metallization layers of Ti:Pt:Au where each metal is 100nm thick. The first 100nm Ti layer absorbs all the pump light passing through the transparent DBR. The experiment and theory results are shown in black and agreement is excellent. The grey curves compare theory and experiment for a thin (nominally 5nm but probably 7nm) Cr layer followed by 100nm Au. The thin CR allows approximately 50% of the pump light to be back-reflected from the Au. We see a very significant increase in slope efficiency although the total extracted power remains the same due to thermal bottlenecking.

Finally, in this section, we show recent results obtained when the 1040nm OPLS chip is pumped by a 775nm pulsed Alexandrite laser. The pulse length is 1μs in this study and repetition rate is 3Hz. Fig. 7 shows a graph of the input peak power at 775nm versus extracted power around 1040nm. The relatively short pump pulse length rules and low repetition rate out significant lattice heating effects but there should ne significant plasma heating under these conditions. Indeed we notice a relatively small shift to long wavelength under these conditions.

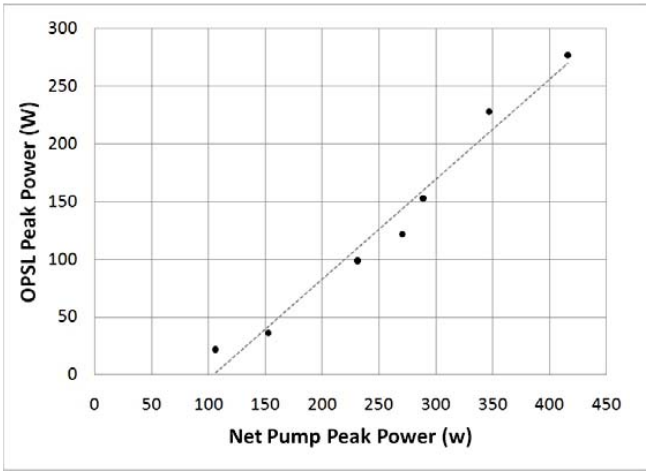

Figure 7. Peak pulsed output power of a 1040nm VECSEL pumped by a 775nm Alexadrite laser with a pulse width of 1 μs.

3. PULSED MID-IR 2μM OPSL

The mid-IR OPSL structure[6,7] here consists of a commercial $Al_{0.95}Ga_{0.05}As$/GaAs distributed Bragg reflector (DBR) with 25 repeats and an antimonide based resonant periodic gain (RPG) region that is monolithically grown on the DBR via an interfacial misfit (IMF) dislocation array[3]. The IMF relaxes the strain due to the lattice mismatch at the GaSb/GaAs interface and eliminates the need for a thick metamorphic buffer to bridge the lattice mismatch between GaAs and GaSb. The RPG region contains nine InGaSb wells separated by pump absorbing AlGaSb barriers.

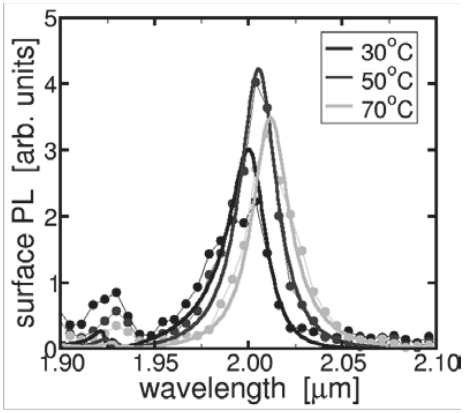

Figure 8. Experimentally measured (thin lines, circles) and microscopically calculated (bold lines) surface-PL spectra at a fixed, low pump power for three temperatures.

The grown structure can be characterized by the surface photoluminescence (PL) and temperature dependent reflectivity spectra at various temperatures. Fig. 8 shows a comparison between the measured PL and

microscopically calculated spectra. Theory and experiment agree very well within the scattering of the experimental data. Both show the same temperature dependent line-shapes, spectral shifts and amplitudes. The maximum amplitude is found for about 50°C. This indicates that for this temperature microcavity resonance and quantum well PL are in resonance.

Figure 9 shows the temperature dependent reflectivity spectra. With a higher temperature, the absorption wavelength of the quantum well and the microcavity resonance both shift to the longer wavelength but with different shift rate. The dip of the curve occurs when the antinodes of the microcavity resonance match the locations of the quantum well. The lasing wavelength is determined by the wavelength for which this reflectivity value is reached for the lowest carrier density. Due to the RPG design, this wavelength is given by the microcavity resonance.

The pump was an active Q-switched Nd:YAG laser generating pulses with duration between 100 – 300 ns. The repetition rate of the pulses was 1 kHz. The laser beam was focused by a 12.5cm focal lens. A linear cavity (see Fig. 10) was used to generate the 2 μm OPSL signal with the output coupler of 10 cm radius of curvature, 6% transmission. 34.2% of the incident pump was lost by Fresnel reflection of the GaSb.

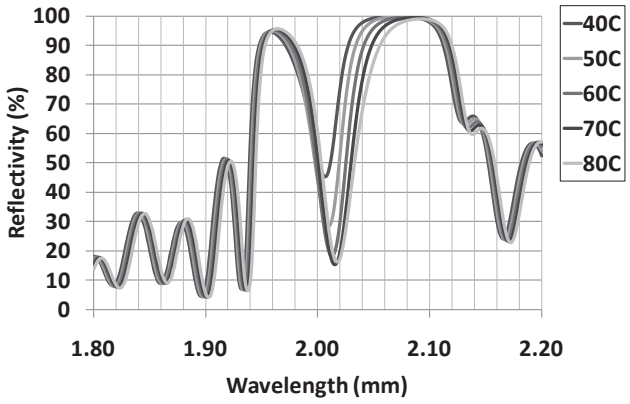

Figure 9. The temperature dependent reflectivity spectra from 40°C to 80°C

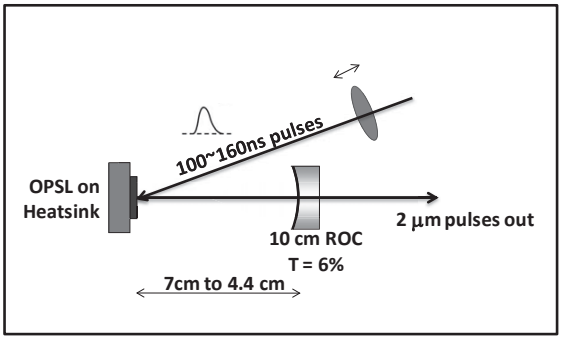

Figure10. OPSL schematic layout. For pulsed pumping.

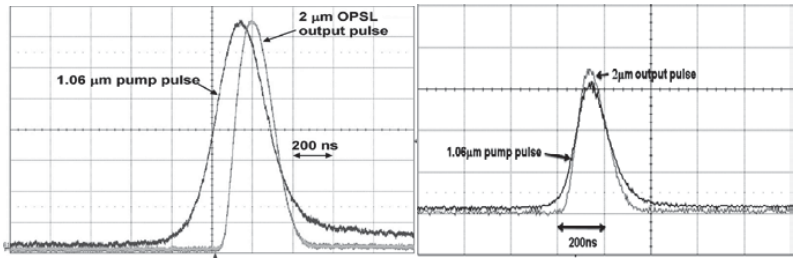

Figure 11. The pulse shape resolved by an oscilloscope when cavity length was 7 cm (left) and 4.4 cm (right).

In addition, the pump spot size can be adjusted by the focal lens, which allows for scaling of the output power by varying spot size. Since the beam size is much larger than the fundamental cavity mode size with a 4.4 cm long linear cavity, the 2 mm beam is highly multi-mode. We calculated the peak power by measuring the average power and dividing by the repetition rate and the pulse width at half maximum. In this experiment, the spot diameter was 0.725mm and 1.4mm and the maximum peak powers were 70W and 342 W, respectively. The power is improved by a factor of 5 while the area of the pump spot is about 5 times larger. To this extent, the results agree well with the power scaling law. When the pump power was further increased with pump spot size of 1.4mm, a maximum output peak power of 378 W was observed with approximately 6 kW pump power, where damage on the OPSL chip occurred.

Thermal effects associated with lattice heating should not play a role here although plasma heating is important. Another significant observation is the power density increases with spot size in contrast to the CW 1040nm OPSL discussed in the last section.

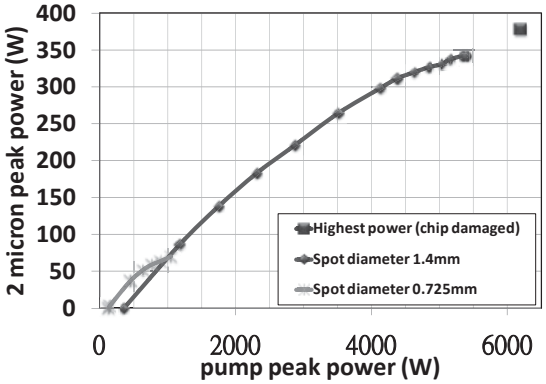

Figure 5. Total incident power vs. output power characteristic for different pump spot diameters: 0.725mm and 1.4mm respectively.

In summary, we have designed a near infrared OPSL with an antimonide-based resonant periodic gain structure grown lattice mismatched on a AlAs/GaAs Bragg mirror, grown samples, and evaluated them under pulsed conditions. We obtained a peak output power over 340 W under ~100 ns pulsed pumping conditions

.

SUMMARY AND FUTURE OUTLOOK

We have presented an overview of the powerful capabilities of a quantum mechanical microscopic many-body approach to design semiconductor QW material systems as the basic building blocks for semiconductor amplifier and laser design. The approach is applied to the design of high power OPSLs here and record CW results are presented at 1040nm and pulsed results at 1040nm and 2μm. The commercial SimuLase software tool is used to design the epitaxial structure (RPG + DBR) and is augmented by using COMSOL and experimental data to provide relevant thermal impedances. While chip processing (mounting and chemical etch substrate removal) are obvious performance limiters, the overriding limitation is heat removal. By growing bottom emitters, we inevitably provide a higher thermal impedance by requiring the heat generated in the active RPG region to flow through the DBR and metallization layers (Ti/Pt/Au + Indium). Despite this we demonstrate record power extraction in CW (64W at 1040nm) and pulsed (245W at 1040nm and 350 W at 2 μm. Simple modifications to double pass the 808nm pump leads to significant increase is slope efficiency by designing a pump transparent DBR and depositing a thin CR adhesion layer prior to depositing a 100nm Au reflective layer.

The quantum design approach can be further extended to longer wavelengths in the mid-IR. For example, a preliminary study confirms that it quantitatively agrees with experimental data at 3.6 μm[8]. Auger processes prove critically important at these longer wavelength making the ability to quantitatively calculate them microscopically crucial.

Acknowledgement: This work was funded by a U.S. Joint Technology Office Multidisciplinary Research Initiative Program Grant No. AFOSR FA9550-07-1-0573.

REFERENCES

1 J. V. Moloney, J. Hader, and S. .W. Koch, “Quantum design of semiconductor active materials: laser and amplifier applications”,Laser & Photon. Rev. Vol.1, 24-43, 2007.

2 J. L. A. Chilla, S. D. Butterworth, A. Zeitschel, J. P. Charles, A. L. Caprara, M. K. Reed, and L. Spinelli, "High-Power Optically Pumped Semiconductor Lasers," *Proc. SPIE*, v 5332, pp 143–150 (2004).

3 S.H. Huang, G. Balakrishnan, A. Khoshakhlagh, A. Jallipalli, L.R. Dawson, and D.L. Huffaker, "Strain relief by periodic misfit arrays for low defect density GaSb on GaAs," Appl. Phys. Lett. 88, 131911 (2006).

4 Simulase™ is marketed by Nonlinear Control Strategies Inc., Tucson. Website: www.nlcstr.com

5 T.-L. Wang, Y. Kaneda, J. M. Yarborough, J. Hader, J. V. Moloney, A. Chernikov, S. Chatterjee, S. W. Koch, B. Kunert, and W. Stolz, “High Power Optically Pumped Semiconductor Laser at 1040 nm”, IEEE Phot. Tech.Letts., v22, 661 (2010).

6 J.M. Yarborough, Yi-Ying Lai, Y. Kaneda, J. Hader, J.V. Moloney, T.J Rotter, G. Balakrishnan, C. Hains, D. Huffaker, and S.W. Koch, "Record pulsed power demonstration of a 2 μm GaSb-based optically pumped semiconductor laser grown lattice-mismatched on an AlAs/GaAs Bragg mirror and substrate, " Appl. Phys. Lett., 95, 081112 (2009).

7 Y.-Y. Lai, J. M. Yarborough, Y. Kaneda, J. Hader, J. V. Moloney, T. J. Rotter, G. Balakrishnan, C. Hains, and S. W. Koch",340-W peak power from a GaSb 2-mm optically pumped semiconductor laser (OPSL) grown mismatched on GaAs" *IEEE Photonics Technology Letters*, vol 22, 1253 (2010).

8 J. Hader, J.V. Moloney, S.W. Koch, I. Vurgaftman, and J.R. Meyer, "Microscopic Analysis of Mid-Infrared Type-II ``W"-Diode Lasers," Appl. Phys. Lett., vol. 94, no. 061106, 2009.